Neuron, Volume *95*

Supplemental Information

The Spatiotemporal Organization of the Striatum Encodes Action Space

Andreas Klaus, Gabriela J. Martins, Vitor B. Paixao, Pengcheng Zhou, Liam Paninski, and Rui M. Costa

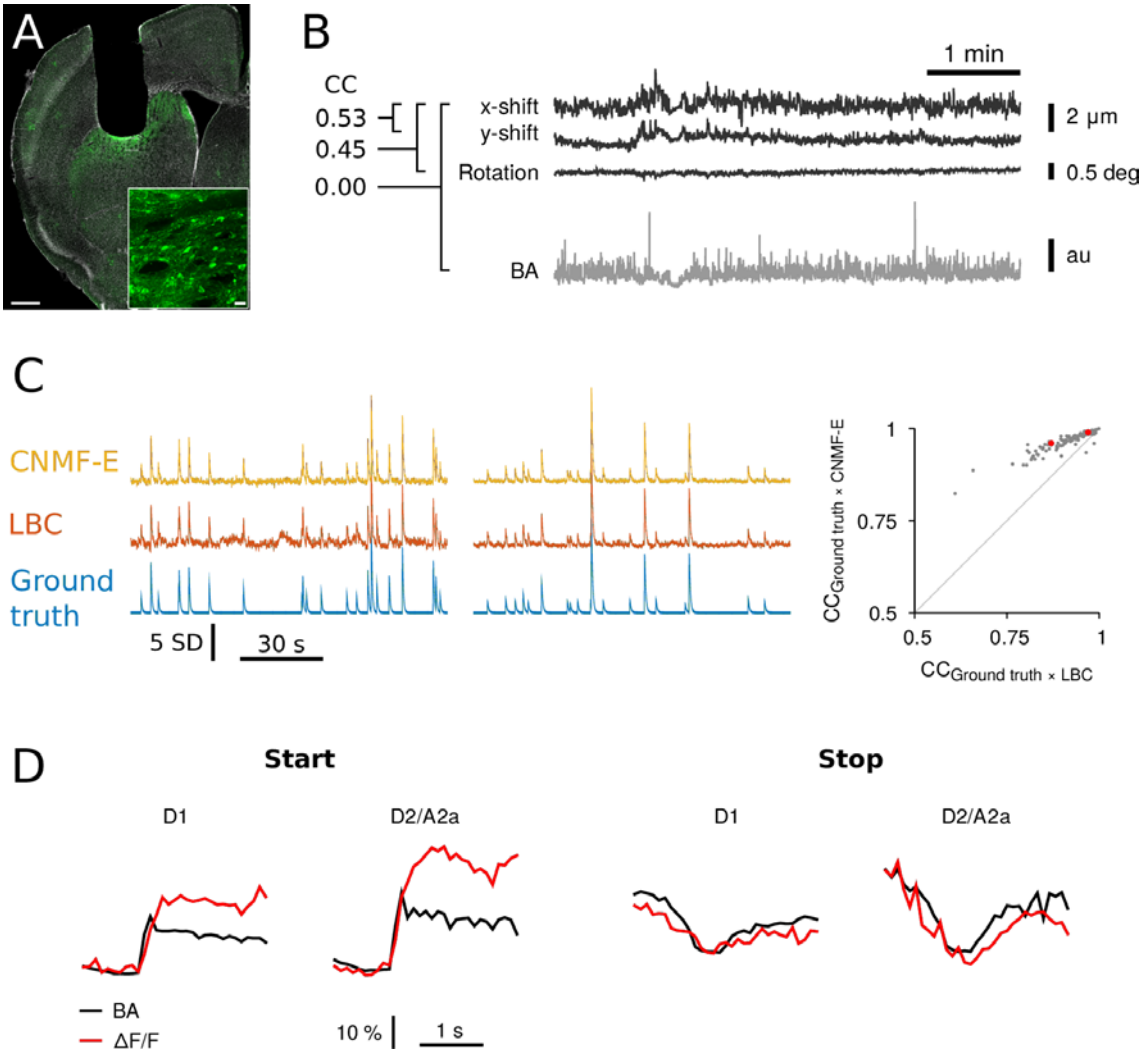

Figure S1: Analysis of one-photon calcium imaging (related to Figure 1). (A) Confocal micrograph of a coronal slice showing the lens placement, injection site and GCaMP6f expression. Scale bars: overview, 500 µm; inset, 20 µm. (B) Image motion is small and not correlated with total body acceleration. Top traces: amount of applied motion correction (x, y-shift and rotation). Motion correction was done using Mosaic software. Bottom: total body acceleration during a time period of movement. CC values were obtained using the entire time series (~10 min). (C) Comparison of LBC and CNMF-E. Left and middle: example traces for two neurons for simulated calcium transients (ground truth, bottom) and reconstructed calcium traces using LBC (middle) and CNMF-E (top). Right: comparison of reconstruction performance of ground truth for LBC and CNMF-E. Reconstruction performance was quantified using CC between the original (simulated ground truth) time series and the reconstructed time series using LBC or CNMF-E, respectively. Higher CC values indicate higher similarity between ground truth and reconstructed time series. The red dots correspond to the two example neurons. Gray line indicates identity. (D) Average calcium activity (ΔF/F obtained with LBC) and BA (arbitrary units, au) during movement start and stop (D1: n=5

mice, D2/A2a: n=5 mice). Movement start was defined as threshold crossing from low to high BA after >500 ms rest followed by >500 ms moving. Movement stop was defined as threshold crossing from high to low BA after >500 ms moving followed by >500 ms rest. The threshold for BA was set to the average value separating the bimodal distribution of BA (visualized in logarithmic scale, see Figure S3A).

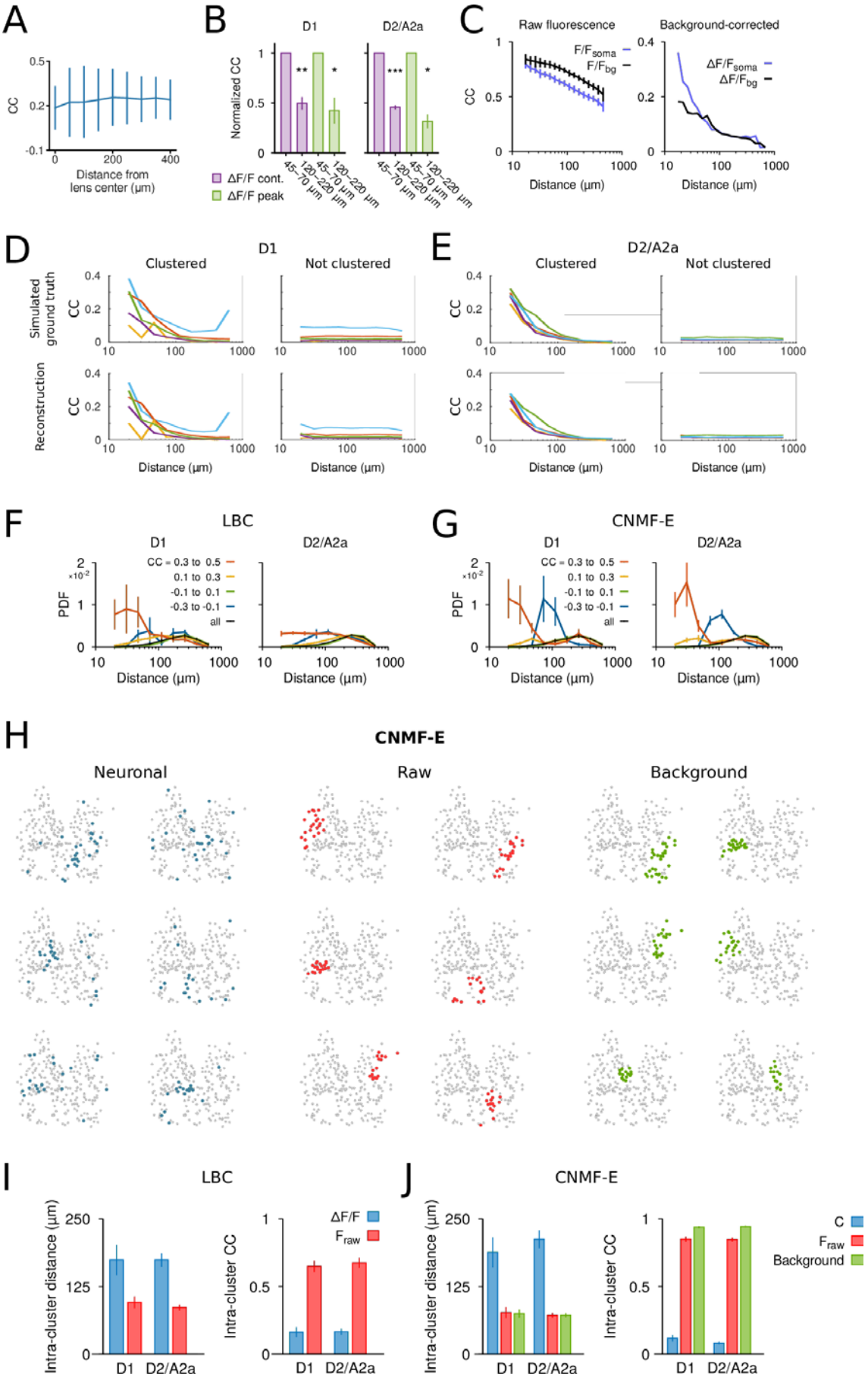
A
CC
Distance from lens center (μm)
B
D1
D2/A2a
Normalized CC
ΔF/F cont.
ΔF/F peak
45–70 μm
120–220 μm
C
Raw fluorescence
Background-corrected
F/Fsoma
F/Fbg
ΔF/Fsoma
ΔF/Fbg
Distance (μm)
D
D1
Clustered
Not clustered
Simulated ground truth
Reconstruction
E
D2/A2a
F
LBC
G
CNMF-E
PDF
CC = 0.3 to 0.5
0.1 to 0.3
-0.1 to 0.1
-0.3 to -0.1
all
H
CNMF-E
Neuronal
Raw
Background
I
LBC
Intra-cluster distance (μm)
Intra-cluster CC
ΔF/F
Fraw
J
CNMF-E
C
Fraw
Background

Figure S2. Spatiotemporal CCs (related to Figure 2). (A) CC estimates were not affected by the image location within the field of view with respect to the center of the lens. For each distance from the lens center, SPNs with up to 70 μm inter-neuronal distance were included. Shown is the average ± standard deviation. (B) A possible confound of the LBC method could be neurons that were not detected by our algorithms but could contribute to the neuronal signals in two nearby neurons. Therefore, CCs were estimated for distances larger than 3 times the average soma diameter (half-width ~14.4 μm, see STAR Methods). CCs were calculated on continuous ΔF/F traces or ΔF/F peak events extracted by thresholding for distances between 45-70 μm and compared to CCs at 120-220 μm. To further minimize possible cross-talk effects, a high threshold for ΔF/F peak detection was chosen, which restricted the analysis to the 20% largest events compared to the 3 SD threshold used for all other analyses. $^{*}p<0.05$, $^{**}p<0.01$, $^{***}p<0.001$. CCs decrease beyond the average soma size. (C) Background signals in experimental data have a different spatial profile than somatic signals. Before 'background correction' (left panel), CCs in the background ROIs (F/F_{bg}) are larger than in the somatic ROIs (F/F_{soma}). CCs were calculated on baseline-subtracted raw calcium traces for the somatic and background ROIs (see STAR Methods). In this analysis, we used the manually selected somatic ROIs from the LBC analysis and the corresponding automatically determined background regions, which show reduced contribution of somatic and neuropil signals in the raw data (i.e., even before any post-processing). After background correction (right panel), CCs in the background ROIs ($\Delta F/F_{bg}$) were smaller than in the somatic ROIs ($\Delta F/F_{soma}$, cf. Figure 2). The small residual in the background CC after background-correction is most likely due to uncorrected residual neuronal signals. The background ROIs were processed in the same way as somatic ROIs, that is, a 'background' was selected within a 2-neuron diameter region around the background and subtracted (see STAR Methods). (D) Reconstruction of CC-distance relationships from simulated ground truth data for D1. Top: CCs calculated from time series including only ΔF/F peak events for the original and spatially shuffled data (n=5 D1 mice; one color per mouse). The ΔF/F peak time series served as the ground truth data for simulated data (see STAR Methods). Bottom: CCs calculated from reconstructed ΔF/F peak time series using the LBC method. The same neuron locations as for the generation of the ground truth data were re-applied, and all steps were performed as described for LBC. (E) Same as *D* for D2/A2a mice (n=5 mice, one color per mouse). (F) Even relatively distant neurons can exhibit strong CCs. Distribution of inter-neuronal distances for various ranges of CC (ΔF/F, LBC). Although strong CCs are predominantly observed for nearby SPNs, increased CCs can be observed at distances larger than 100 μm. (G) Same as *F* for calcium activities obtained with CNMF-E. (H) Neuronal clusters cover overlapping regions and are spatially not compact. Clusters obtained from neuronal (i.e., somatic), raw, and background signals. Only raw and background time series result in spatially compact clusters. Clusters were sorted by number of neurons within the cluster (first six clusters shown for each condition). (I) Distance and CC between ROIs within clusters ("intra-cluster"). In contrast to raw fluorescence (F_{raw}) signals, neuronal (ΔF/F, LBC) signals resulted in clusters with increased intra-cluster distance and low average CC. To restrict analysis to the same spatial locations, LBC background was not analyzed. Clusters with at least 5 neurons were included in the average (D1: n=5 mice, D2/A2a: n=5 mice). (J) Same as *I* for CNMF-E. The 'raw' and 'background' signals for each neuron were extracted from the raw data and CNMF-E background, respectively, using the spatial footprint of the neuron.

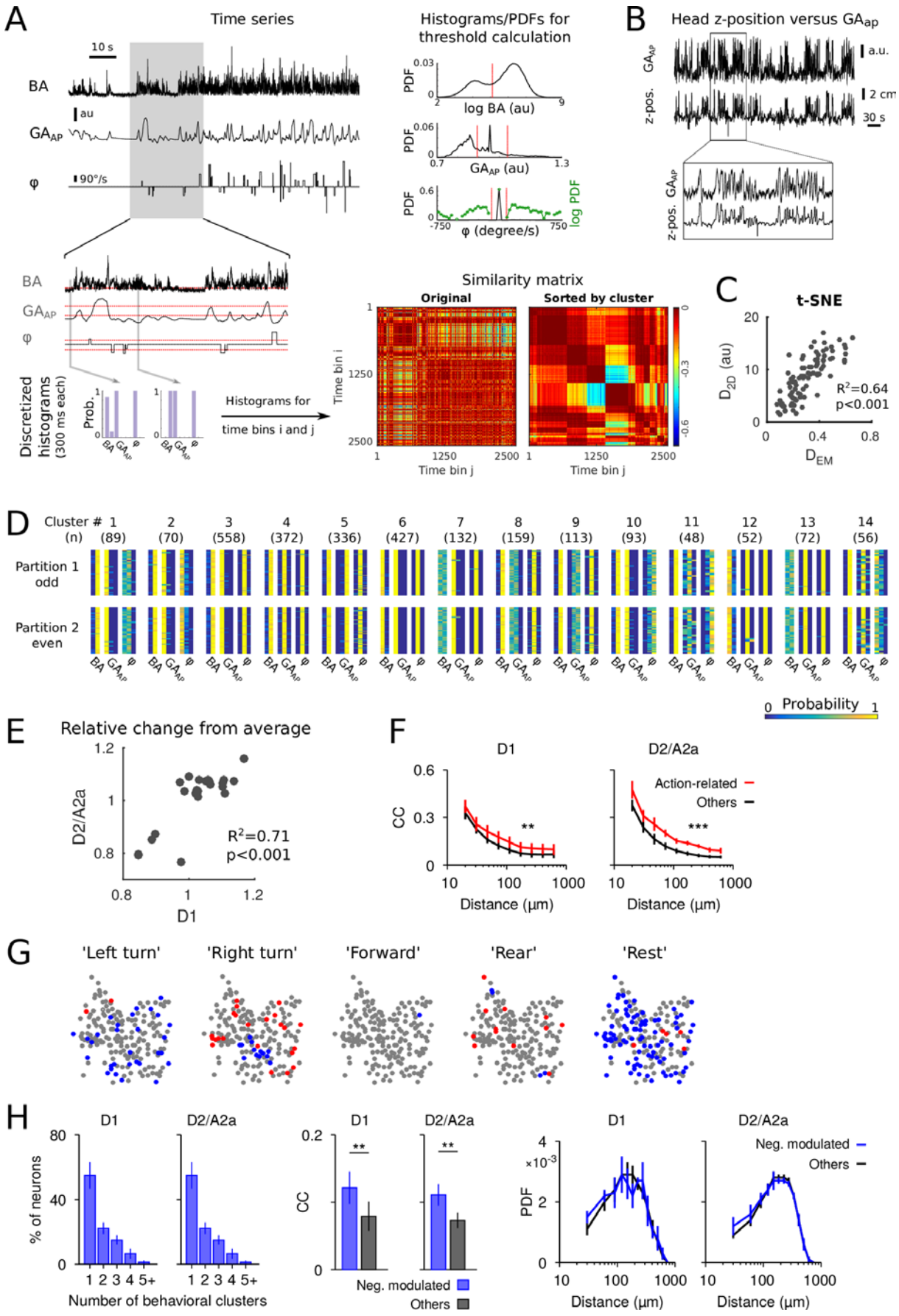
A
Time series
10 s
BA
au
GA_AP
φ
90°/s
Histograms/PDFs for threshold calculation
PDF
log BA (au)
GA_AP (au)
φ (degree/s)
log PDF
Discretized histograms (300 ms each)
Prob.
Histograms for time bins i and j
Similarity matrix
Original
Sorted by cluster
Time bin i
Time bin j
B
Head z-position versus GA_ap
z-pos.
a.u.
2 cm
30 s
C
t-SNE
D_2D (au)
D_EM
R²=0.64
p<0.001
D
Cluster # (n)
1 (89)
2 (70)
3 (558)
4 (372)
5 (336)
6 (427)
7 (132)
8 (159)
9 (113)
10 (93)
11 (48)
12 (52)
13 (72)
14 (56)
Partition 1 odd
Partition 2 even
Probability
E
Relative change from average
D2/A2a
D1
R²=0.71
p<0.001
F
D1
D2/A2a
Action-related
Others
CC
Distance (μm)
G
'Left turn'
'Right turn'
'Forward'
'Rear'
'Rest'
H
% of neurons
Number of behavioral clusters
Neg. modulated
Others
PDF

Figure S3: Behavioral clustering algorithm (related to Figure 3). (A) Time series (top, left) and corresponding PDFs with thresholds (top, right) for BA, GA_{AP}, and φ. The thresholds (red lines) are shown together with a detailed view of the time series (middle, left) and the discretized distributions for two 300-ms time bins (bottom, left). Bottom, right: a matrix of pairwise similarities between the discretized histograms is shown for time bins in the original order and sorted by behavioral cluster. (B) Gravitational acceleration in the anterio-posterior axis correlates with vertical head movements. GA_{AP} is highly correlated with the height (z-position) of the mouse's head during freely moving open field behavior (CC=0.87, $p<0.001$). Large values of the z-position correspond to periods of rearing. (C) The distances in the two-dimensional projection obtained with t-SNE (D_{2D}, cf. Figure 3C) reliably reflect the EM-distances as quantified using linear regression. (D) Discretized histograms (each corresponding to 300 ms behavioral data) are shown for partitioned data. Histograms are sequentially numbered according to their time bin, and partition 1 and 2 correspond to all odd- and even-numbered histograms, respectively. This partitioning was used for control analyses using cross-validated Euclidean distance (see STAR Methods). Cluster numbers and number of samples *n* (in parentheses) are shown at the top. (E) Relative change of average ΔF/F during 'matched' behavioral clusters was similar for D1 and D2/A2a (quantified using linear regression). Behaviors were matched against a library of 75 pre-defined behaviors covering a homogeneous 'action space'. (F) CC-distance relationship shows increased CCs between 'action-related' SPNs compared to 'other' SPNs at all inter-neuronal distances. Statistical comparison was performed on the average CC and is replicated from Figure 3F (top). (G) Example neuronal maps showing significantly positively (i.e., 'action-related') SPNs (red), significantly negatively modulated SPNs (blue) and non-significant SPNs (gray). The majority of behavioral clusters had fewer than 20% of neurons being either significantly positive or negatively modulated (percentage of behavioral clusters for D1: pos. 90%, neg. 84%; for D2/A2a: pos. 97%, neg. 87%). (H) Analysis of negatively modulated SPNs. Left: percentage of negatively modulated neurons that show significant modulations for 1, 2, 3, 4, or 5 and more behavioral clusters. Middle: average CC for significantly negatively modulated and all other neurons. Right: corresponding PDF for inter-neuronal distances shows no significant difference between negatively modulated and other SPNs (D1: n=5 mice, p=0.341; D2/A2a: n=5 mice, p=0.185). Panels E-H are shown for LBC. For the analysis of positively modulated (i.e., 'action-related') SPNs, see Figure 3E-G.

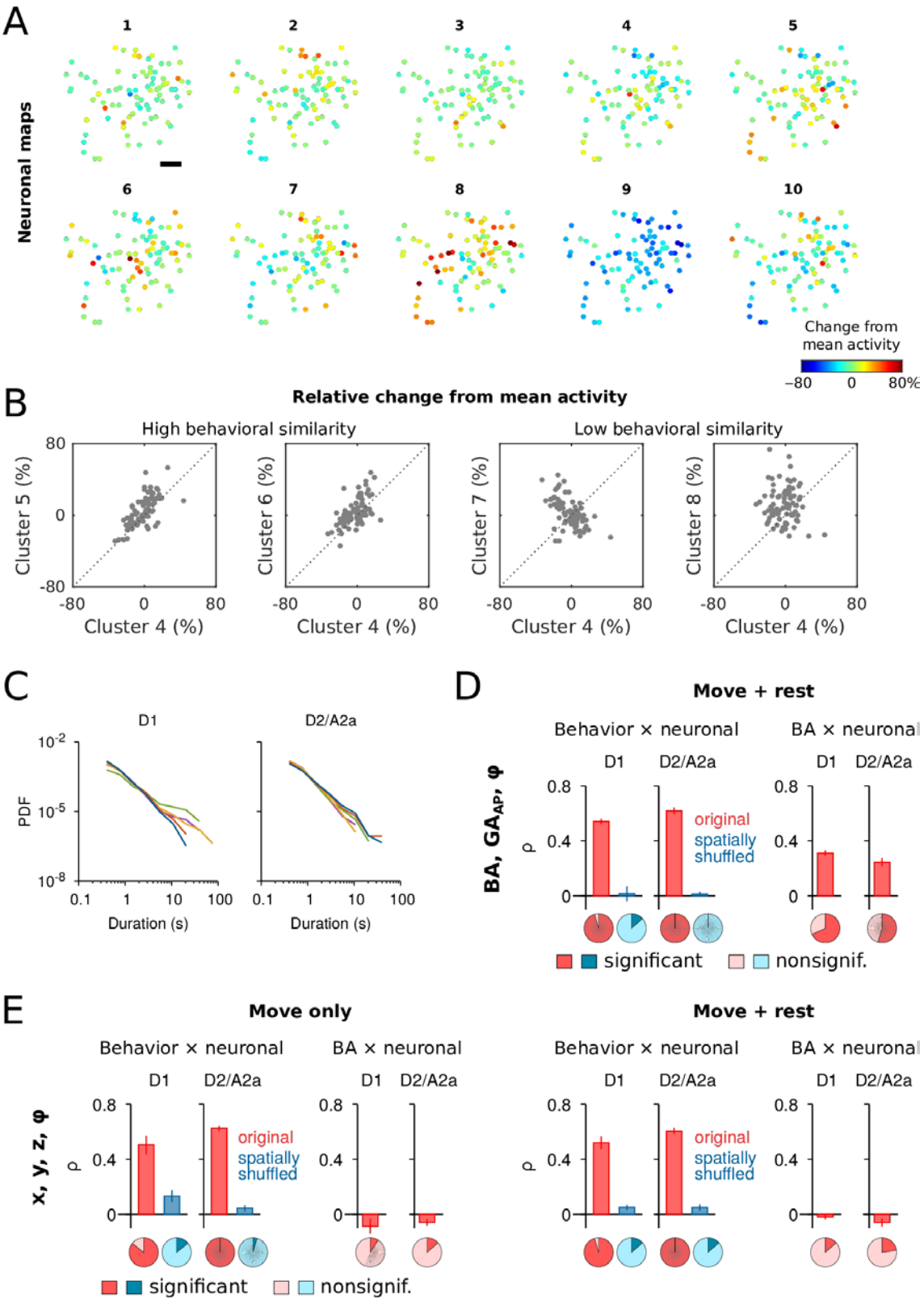

Figure S4: SPN activity during distinct behavioral clusters (related to Figure 4). (A) Neuronal maps for a D1 example session showing, for each behavior cluster, the relative changes in activity compared to each neuron's mean activity and the neuron positions in the field of view. Scale bar: 100 µm. (B) Comparison of relative activity changes between behavioral cluster 4 and clusters 5-8 (ordered from left to right by decreasing behavior similarity). Each dot corresponds to a single SPN. (C) Durations of behavioral segments range from sub-second to tens of seconds. PDFs of behavioral

segment duration (multiples of the behavioral bin size, 300 ms) for all D1-Cre and D2/A2a-Cre mice (D1: n=5; D2/A2a: n=5 mice, one color per mouse). Data is visualized in double-logarithmic scale for better visualization. (D) Left: average correlation, ρ, between behavioral and neuronal similarity for all behavioral clusters (i.e., moving and resting). Right: corresponding correlation between BA similarity and neuronal similarity. (E) Behavioral and neuronal similarities are correlated also for more general movement features, that is, time series of median-filtered raw acceleration (x, y, and z) and head/body rotation. Left: quantification for behavioral clusters with movement (i.e., resting clusters excluded, see STAR Methods). Right: quantification for all behavioral clusters (i.e., moving and resting). The pie charts in *D* and *E* show the percentage of sessions with significant *versus* nonsignificant correlation values.